

ACCELERATED FULLY 3D ITERATIVE RECONSTRUCTION IN SPECT

Werner Backfrieder^(a), Gerald A. Zwettler^(b)

^{(a), (b)}University of Applied Sciences Upper Austria, Institute of Software Engineering, Campus Hagenberg, Austria

^(a)Werner.Backfrieder@fh-hagenberg.at, ^(b)Gerald.Zwettler@fh-hagenberg.at

ABSTRACT

Image quality in single photon emission computed tomography (SPECT) is substantially influenced by scatter and a finite volume of response associated with single detector elements. These effects are not restricted to the image plane, implying a shift in the tomographic imaging paradigm from 2D to 3D. The application of a 3D reconstruction model suffers from huge numerical efforts, affording for high performance computing hardware. A novel accelerated 3D ML-EM type reconstruction algorithm is developed by the implementation of a dual projector back-projector pair. An accurate 3D model of data acquisition is developed considering scatter and exact scanner geometry in opposite to a simple pencil-beam back-projection operator. This dual concept of projection and back-projection substantially accelerates the reconstruction process. Speed-up factors achieved by the novel algorithm are measured for several matrix sizes and collimator types. Accuracy of the accelerated reconstruction algorithm is shown by reconstruction of data from a physical Jaszczak phantom and a clinical endocrine study. In both cases the accelerated 3D reconstruction method achieves better results. The novel algorithm has a great potential to scale fully 3D reconstruction down to desktop applications, especially with the new possibilities employing massive parallel graphics hardware. The presented work is a step towards establishing sophisticated 3D reconstruction in a clinical workflow.

Keywords: emission tomography, fully 3D reconstruction, nuclear medicine, high-performance computing

1. INTRODUCTION

Nuclear medicine imaging modalities show the distribution of radioactive tracer providing diagnostic information. Main fields of application are tumor diagnostics and in vivo assessment of metabolism. Therapeutic applications are limited to therapy with beta-emitters, e.g. radioiodine therapy of the thyroid. In nuclear medicine imaging the kinetics of radioactive tracer particles within the human body is the basis of diagnostic information. After intravenous application specialized radiopharmaceuticals distribute within the body and finally accumulate in targeted morphological

regions. In tumor diagnosis tissue pathologies are imaged as hot spots. The amount of activity uptake and the size of the lesion are an important measure for the progress of the tumor disease. Both, distribution and kinetics of the radiotracer are subject to functional imaging, e.g. perfusion images of the human brain after stroke or assessment of the clearance rate in kidneys.

Single photon emission computed tomography (SPECT) is a volume imaging technique, visualizing the human body as a series of transversal slices. The photons generated during disintegration of a short lived radionuclide, e.g. Tc-99m, are registered by a gamma-camera as projection images. There is a great variety of algorithms for the reconstruction transversal slices from projection data. Filtered back-projection (FBP) in combination with specific filter windows is, due to its high performance, the main method in clinical practice (Herman 2009). With increasing computational power iterative methods, allowing a more accurate modeling of geometrical and physical properties of the imaging process, were introduced into clinical environments. The maximum likelihood expectation maximization (ML-EM) algorithm (Shepp and Vardi 1982) is the foundation of a series of optimized algorithms in emission tomography (Hudson and Larkin 1994).

The slice topology of the reconstruction algorithms is a major limitation in image quality of emission tomography. In contrast to x-ray computed tomography the scanner hardware allows major interferences from adjacent slices. Collimator geometry defines a conic volume of response to a single detector position; low count rate and scatter are major deteriorating effects in SPECT imaging. Fully 3D image reconstruction accomplishes the simultaneous reconstruction of the whole image volume, but at the cost of high computational burden (Backfrieder et al. 2002, Backfrieder et al. 2003a, Backfrieder et al. 2003b, Benkner et al. 2004).

In the following a fully 3D iterative reconstruction algorithm is described implementing a dual projector back-projector pair for accelerated reconstruction. The newly developed algorithm is based on the OS-EM family providing accelerated convergence (Hudson and Larkin 1994).

2. MATERIAL AND METHODS

The imaging equation in tomography reads

$$y_i = \sum_j a_{ij} \cdot x_j + e_i, \quad (1)$$

it describes the relation between the pixels of the source distribution (=image) x and a single projection values y . Both, the image and projection array are two-dimensional, i.e. x -and y -direction in the image, angle and lateral distance in projections, but are represented by a single linear index. A value of the system matrix a_{ij} describes the contribution of pixel x_j to the projection value y_i . This allows the accurate modeling of

- scanner geometry
- photon attenuation
- detector response
- scatter

Figure 1 shows a sketch of the image plane and the pixels summing up a single projection value.

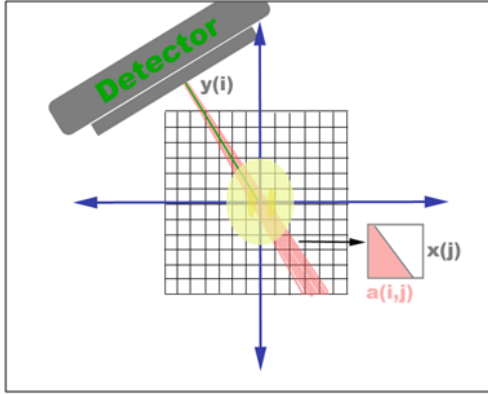


Figure 1: Sketch of SPECT scanner geometry.

Each measured value contains an error term e_i . In the case of radioactive decay and detection of photons this error term is Poisson-distributed. Under the constraint of a Poisson-distributed random process image reconstruction is formulated as a maximization problem of the likelihood L of measured data y

$$L(y | x) = \prod_i \frac{\left(\sum_j a_{ij} \cdot x_j \right)^{y_i} e^{-\sum_j a_{ij} \cdot x_j}}{y_i!}, \quad (2)$$

where the sum represents the expectation value of the respective measured projection value y_i . The algorithm aims in maximizing the term in Eqn. 2 by choosing a proper image-vector \mathbf{x} . The solution is the iterative ML-EM algorithm for tomography by Shepp and Vardi, 1982

$$x_j^{(n+1)} = x_j^{(n)} \sum_i a_{ij} \frac{y_i}{\sum_{j'} a_{ij'} x_j^{(n)}}. \quad (3)$$

A sequence of intermediate images $x^{(n)}$ is calculated until a stopping criterion is satisfied. During the n^{th} iteration each pixel x_j is updated by a multiplicative factor. This factor is the weighted sum of all projection values y_i affected by the pixel x_i . The correction term depends on the quotient of the measured projection value and the calculated pseudo-projection

$$y_i^p = \sum_{j'} a_{ij'} x_j^{(n)}. \quad (4)$$

The iteration steps in Eqn. 3 converge to a feasible solution, representing a maximum entropy solution to the imaging equation. To further accelerate the convergence of the algorithm ordered subsets are implemented.

The discussed reconstruction model describes the reconstruction of a single image slice. Spatial activity distribution out of the slice is not considered by this model. Finite collimator aperture and scatter have significant contribution from pixels out of the considered slice on the projection values, necessitating a three dimensional (3D) approach to the reconstruction problem for further improvement of image quality. In contrast to FBP the iterative approach allows a simple extension to 3D by covering the whole image volume and projection values of all slices by respective vectors. As a consequence the system matrix A grows $o(N^6)$ with the lateral length (N pixels) of the image cube.

2.1. Modeling of the system matrix

Each line of the system matrix defines the weights of all voxels to a specific projection value. In a conventional SPECT study the image volume consists of 128 slices, with a matrix size of 128x128 pixels, each. A row consists of $128^3=2.097.152$ elements. The number of projection values, i.e. the number of lines of the matrix, is calculated from the size of the projection matrix and the angular increment of the detector head, i.e. 128x128x120 for a 3 degrees increment on a circular orbit. In total the system matrix contains 4.12×10^{12} elements. Even dedicated high-performance-computer (HPC) systems cannot hold this huge amount of data in memory.

Since a line of the system matrix considers all elements of the image volume, most of the entries are zero. With careful modeling of the geometrical and physical properties of data acquisition, this leads to a significant reduction of data.

Each projection value is related to a flat rectangular region of the detector surface, i.e. the field of view (FOV) divided by the number of elements of the projection matrix. For assessment of the contribution of each voxel to a specific projection value, a point source is positioned at the center of a voxel and the fraction of radiation reaching the detector element is calculated. This corresponds to the ratio of the surface of a sphere, with origin in the voxel and the radius is the distance to the detector element, and the projection of this detector element onto this sphere. This simple geometrical

consideration leads to a model of the volume of response as a cone targeting to the detector surface. With increasing distance to the detector the cone-width increases and the weight of voxels decreases. The voxel weights at the level of the central slice of the volume of response (VOR), i.e. at the level of the projection value, are shown in Fig. 2.a. The VOR has circular symmetry.

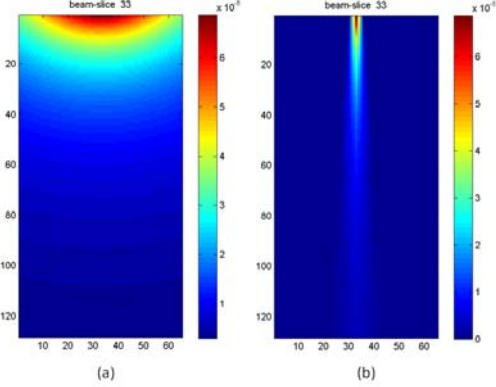


Figure 2: Volume of response of a 128x128 projection matrix (a) and its amplification by a LEGP collimator (b).

The camera head is equipped with a lead collimator, to limit the viewing direction approximately to bars normal to the detector surface. The design consists of a regular pattern of thin lead septa, arranged as long thin bore holes or as a honeycomb grid. The modulation factor is the cast shadow of the collimator septa depending on the detector thickness and the ratio of wall thickness of septa and their aperture. Scatter is a further amplification of the voxel weights; usually it is modeled by a zero centered Gaussian distribution. The total pixel weight reads

$$a_{ij} = \Theta_{scatter} \alpha_{coll} \Phi_{geom}, \quad (5)$$

where the geometrical form factor is Φ , the attenuation factor of the collimator is α and the contribution of photon scatter by human tissue is Θ . Figure 2.b shows the application of the collimation factor to the VOR.

2.2. Dual projector back-projector pair

In the previous section the OS-EM algorithm and the modeling of the system matrix is discussed in detail. With the generalization of the reconstruction problem to 3D the computational effort increases substantially, affording for HPC hardware to achieve suitable performance for image reconstruction, to establish it in a clinical environment.

The high cost of the ML-EM algorithm is caused by a series of projections and back-projections during each iteration step, cf. Eqn. 3. The sum over all projection values containing the actual pixel can be considered as back-projection. From each intermediate image $x^{(n)}$ pseudo-projections are calculated. The number of

numerical operations is proportional to the non-zero elements of the system-matrix \mathbf{A} . To achieve most accurate physical and geometrical modeling the forward projection is implemented by the modeled weights according to Eqn. 4. The accurate assessment of pseudo-projections is crucial, since its ratio to measured projection values y_i defines the amount of the correction term. The back-projection operator comprises the projection values considered for the update of a specific pixel. In this novel approach not all elements, as defined by the above model of the system matrix, are considered, but only a subset defined by orthogonal projection onto the detector surface. The lateral distance from the center of the profile is

$$l = x \cdot \cos \mathcal{G} + y \cdot \sin \mathcal{G}, \quad (6)$$

where x, y are the coordinates of the updated voxel and \mathcal{G} is the rotation angle of the detector head. Only projection values within the slice are considered. The ML-EM algorithm with dual projector and back-projector pair reads

$$x_j^{(n+1)} = x_j^{(n)} \sum_i l_{ij} \frac{y_i}{\sum_{j'} a_{ij'} x_{j'}^{(n)}}. \quad (7)$$

The coefficients l_{ij} denote the reduced set of back-projection values. The speed up factor is linear to the reduction of the l_{ij} coefficients in relation to the total number of entries in the system matrix entries a_{ij} . For a standard 128x128 matrix and a LEGP parallel collimator the speed-up factor is 218.53. This speed up of fully 3D reconstruction implemented together with the ordered subsets concept, the newly developed algorithm is called 3D accelerated ordered subsets expectation maximization (3D-AOS-EM).

2.3. Physical phantom and patient data

Data are collected from a circular clinical standard Jaszczak SPECT phantom on a three headed Philips IRIX camera. The phantom was filled with 600 MBq Tc-99m. Acquisition parameters were: 128 by 128 projection matrix, pixel size 4.4mm, 120 projections on a full circular orbit of 360 degrees and 20s acquisition times in stop and go mode.

On the same camera data from a clinical endocrine study, 55MBq I-131 applied activity, were acquired on a 64 by 64 projection matrix over a 565mm FOV, with 60 projections on a circular orbit, and 30s acquisition time per projection.

3. RESULTS

Results are shown for acceleration of the algorithm in contrast to 3D ML-EM, a comparison of reconstruction methods applied to physical phantom data and a clinical study.

3.1. Speed up factors

The speed-up factors - as a consequence of the implementation of the accelerated back-projection operator - are shown in Figure 3. Results are shown for two collimator types, a low energy general purpose (LEGP) and a high energy high resolution (HEHR) collimator. The speed up factor directly relates to the reduction of entries in the back-projection matrix compared to those in the respective projection matrix, as shown by different factors for the collimators used during the studies. The HEHR collimator has a significantly smaller VOR thus the speed-ups are smaller than those of the LEGP collimator, cf. Fig. 3.

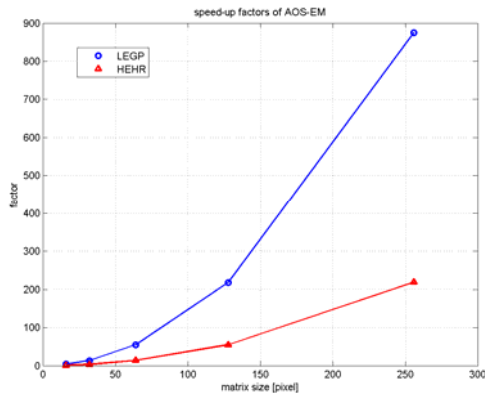


Figure 3: Speed-up factors

3.2. Phantom data

A slice of the Jaszczak phantom comprising 6 sectors of cold rods with increasing diameter is shown in Fig. 4. Slices were reconstructed using FBP, the clinical standard, and the accelerated fully 3D reconstruction with dual projection back-projection (3D-AOS-EM). During iterative reconstruction 15 iterations with 4 subsets were performed. Compared to FBP the contrast of cold spots is significantly increased with 3D-AOS-EM. In sector 4 (numbered in order of decreasing diameter) rods are still distinguishable, especially in the distal part of the phantom, since with FBP the whole sector is blurred out.

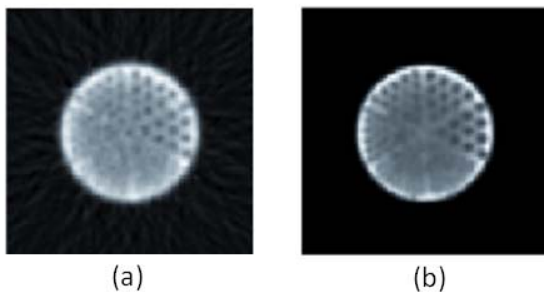


Figure 4: Reconstruction of a standard Jaszczak phantom using (a) FBP and the novel 3D-AOS-EM algorithm.

3.3. Clinical data

Data from the clinical study show a transversal slice through the thyroid, cf. Fig. 5. FBP suffers from low

signal intensity, manifested by substantial star-artifacts centered at the lesion. The hot lesion is a connected oval region with a small tail at the lower left. This image data cannot clearly support the decision, if this tiny image structure is a real pathology or an artifact. 2D-ML-EM reconstruction shows a clearly manifested hot lesion in this part of the image. Reconstruction of the image using the newly developed 3D-AOS-EM yields two clearly distinguishable hot lesions.

4. DISCUSSION

Fully 3D image reconstruction is the most accurate reconstruction model for nuclear medicine emission tomography. The direct implementation of the 3D data model suffers from high computational complexity resulting in long reconstruction cycles, hardly to establish in a clinical workflow. The substantial acceleration of the algorithm by introduction of a dual projector back-projector pair has high potential to scale down the problem from HPC platforms, as already implemented on PC-clusters (Backfrieder et al. 2003b), to desktop hardware. The actual algorithm is implemented as a MATLAB prototype, thus the evaluation of the performance is done on basis of speed-up factors. The newly introduced programming interface CUDA to the highly parallel architecture of the graphics-subsystem offers new perspectives to solve computationally intensive numerical problems. In ongoing work the 3D-AOS-EM algorithm will be implemented in the C-CUDA framework.

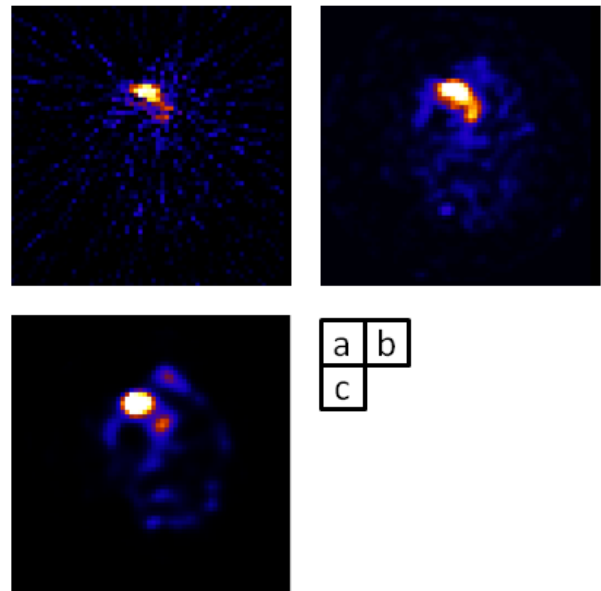


Figure 5: Endocrine study reconstructed FBP (a), 2D-ML-EM (b) and 3D-AOS-EM.

The acceleration of the fully 3D reconstruction together with its implementation on desktop systems is a further step towards sophisticated image processing supporting clinical diagnostics.

ACKNOWLEDGMENTS

Authors want to thank Univ.-Prof. Dr. Michael Gabriel and the radiological technologist from the Institute of Endocrinology and Nuclear Medicine of the General Hospital Linz, Austria, for providing SPECT data.

REFERENCES

- Backfrieder, W., Forster, M., Benkner, S., Engelbrecht, G., Terziev, N., Dimitrov, A., 2002. Accurate attenuation correction for a fully 3D reconstruction service. *Proceedings of the International Conference on Mathematics and Engineering Techniques in Medicine and Biological Sciences (METMBS '02)*, Las Vegas, Nevada, USA, June 24 – 27, 2002: 680-685
- Backfrieder, W., Forster, M., John, P., Engelbrecht, G., Benkner, S., 2003a. Fully 3D Iterative SPECT Reconstruction in A High Performance Computing Environment. *J. Nucl. Med. Technol. Vol.31 No.6*, pp. 201
- Backfrieder, W., Forster, M., Engelbrecht, G., Benkner, S., 2003b. Locally variant VOR in fully 3D SPECT within a service oriented environment. In F. Valafar, H. Valafar (Eds.), *Proc. Int. Conf. on Mathematics and Engineering Techniques in Medical and Biological Sciences (METMBS)*, ISBN 1-932415-04-1, (2003) pp. 216-221
- Benkner, S., Engelbrecht, G., Backfrieder, W., Berti, G., Fingberg, J., Kohring, G., Schmidt, J.G., Middleton, S.E., Jones, D., Fenner, J., 2004. Numerical Simulation for eHealth: Grid-enabled Medical Simulation Services. In G.R. Joubert, W.E. Nagel, F.J. Peters, W.V. Walter (Eds.), *Software Technology, Algorithms, Architectures and Applications, included in series: Advances in Parallel Computing*, Elsevier (2004)
- Herman, G. T., 2009. *Fundamentals of computerized tomography: Image reconstruction from projections*, 2nd edition, Springer, 2009
- Hudson, H.M., Larkin, R.S., 1994. Accelerated image reconstruction using ordered subsets of projection data. *IEEE Trans Med Imaging*. 1994;13:601–609.
- Shepp, L.A., Vardi, Y., 1982. Maximum likelihood estimation for emission tomography. *IEEE Trans Med Imag*. 1982;MI-1(2):113–121.

AUTHORS BIOGRAPHY

Werner Backfrieder received his degree in technical physics at the Vienna University of Technology in 1992. Then he was with the Department of Biomedical Engineering and Physics of the Medical University of Vienna, where he reached a tenure position in 2002. Since 2002 he is with the University of Applied Sciences Upper Austria at the division of Biomedical Informatics. His research focus is on Medical Physics and Medical Image Processing in Nuclear Medicine and Radiology with emphasis to high performance computing. Recently research efforts are laid on virtual

reality techniques in the context of surgical planning and navigation.

Gerald A. Zwettler was born in Wels, Austria and attended the Upper Austrian University of Applied Sciences, Campus Hagenberg where he studied software engineering for medicine and graduated Dipl.-Ing.(FH) in 2005 and the follow up master studies in software engineering in 2009. In 2010 he started his PhD studies at the University of Vienna at the Faculty of Computer Sciences. Since 2005 he is working as research and teaching assistant at the Upper Austrian University of Applied Sciences at the school of informatics, communications and media at the Campus Hagenberg in the field of medical image analysis and software engineering with focus on computer-based diagnostics support and medical applications.